Cell, Vol. 92, 161–171, January 23, 1998, Copyright ©1998 by Cell Press

Simultaneous Observation of Individual ATPase and Mechanical Events by a Single Myosin Molecule during Interaction with Actin

Akihiko Ishijima,*† Hiroaki Kojima,* Takashi Funatsu,* Makio Tokunaga,* Hideo Higuchi,* Hiroto Tanaka,‡ and Toshio Yanagida*‡§
*Biomotron Project
ERATO
JST
Mino, Osaka 562
Japan
†Wako Research Center
HONDA R&D Company
Wako, Saitama
Japan
‡Department of Physiology
Osaka University Medical School
Suita, Osaka
Japan

Summary

We have developed a technique that allows mechanical and ligand-binding events in a single myosin molecule to be monitored simultaneously. We describe how steps in the ATPase reaction are temporally related to mechanical events at the single molecule level. The results show that the force generation does not always coincide with the release of bound nucleotide, presumably ADP. Instead the myosin head produces force several hundreds of milliseconds after bound nucleotide is released. This finding does not support the widely accepted view that force generation is directly coupled to the release of bound ligands. It suggests that myosin has a hysteresis or memory state, which stores chemical energy from ATP hydrolysis.

Introduction

Muscle contraction and many other forms of cellular motion are propelled by an actin-based molecular motor, myosin, driven by the chemical energy of ATP hydrolysis. To elucidate the mechanism of motion underlying the myosin motor, it is crucial to determine how the ATPase reaction is coupled to the mechanical reaction during force generation. However, despite much investigation, this problem has remained unsolved. Recently, much attention has been focused on motility assays, which utilize purified motor proteins in vitro, to probe the elementary mechanical and chemical processes directly at the molecular level.

In vitro motility assays allow the direct observation by optical microscopy of single actin filaments labeled with fluorescent phalloidin (Yanagida et al., 1984), as well as the motion produced by myosin molecules bound to artificial surfaces (Kron and Spudich, 1986; Harada et al., 1987; Toyoshima et al., 1987), and have substantially aided the progress of research on the myosin motor (H.E. Huxley, 1990). Furthermore, a very subtle technique for manipulating a single actin filament with a fine glass needle has been developed (Kishino and Yanagida, 1988), allowing the measurement of both the motion and force of individual myosin motors in vitro at very high (subnanometer) displacement and (subpiconewton) force resolution (Ishijima et al., 1991). We have recently extended this high-resolution manipulation technique to measure the force and displacement directly from single myosin molecules (Ishijima et al., 1994, 1996). Alternatively, a laser trap can be used to manipulate motor proteins attached to spherical particles with a diameter of several hundred nanometers (Simmons et al., 1993; Svoboda et al, 1993). Using this method, the individual mechanical events have been measured directly from single myosin subfragment 1 and heavy meromyosin molecules (Finer et al., 1994; Miyata et al., 1994; Molloy et al., 1995; Guilford et al. 1997).

We have recently demonstrated that single fluorophores can be observed in aqueous solution in real time by total internal reflection fluorescence microscopy, refined so that the background noise is very low (Funatsu et al., 1995; Vale et al., 1996, Harada et al., 1997). This technique has been extended to detect individual ATP turnovers of a myosin molecule by observing single association-dissociation events of a fluorescent ATP analog, Cy3-ATP (Funatsu et al., 1995; Iwane et al., 1997; Tokunaga et al., 1997). Fluorescent ATP analogs, in which the ribose is fluorescently labeled, are a good substrate for myosin as determined by the nucleotidase activity and actin motility (Conibear et al., 1996; Eccleston et al., 1996; Tokunaga et al., 1997).

In this study, we have developed an assay for simultaneously measuring individual ATPase and mechanical reactions of single myosin molecules during force generation by combining the techniques for single molecule imaging and nanomanipulation. This assay shows how the ATPase reaction corresponds to the mechanical reaction in the myosin molecular motor. We have shown that a myosin head can still produce force several hundred milliseconds after releasing the bound nucleotide, suggesting that the myosin head has a hysteresis state, which stores chemical energy from ATP hydrolysis. This view differs from many current models for mechanochemical energy transduction in which the force generation is coupled precisely to a change in ligand (release of ADP and/or Pi) bound to the myosin head (Lymn and Taylor, 1971; Goldman, 1987; Rayment et al. 1993b; Fisher et al. 1995; Yount et al. 1995). These results will prove fundamental not only for understanding the mechanism of mechanochemical energy transduction in molecular motors but also for understanding the general mechanisms of allosteric effects (Monod, et al., 1965).

Results

Measurement System

Figures 1A and 1B depict the experimental system for simultaneously measuring ATPase and mechanical reactions by individual myosin heads. The system was

§To whom correspondence should be addressed.

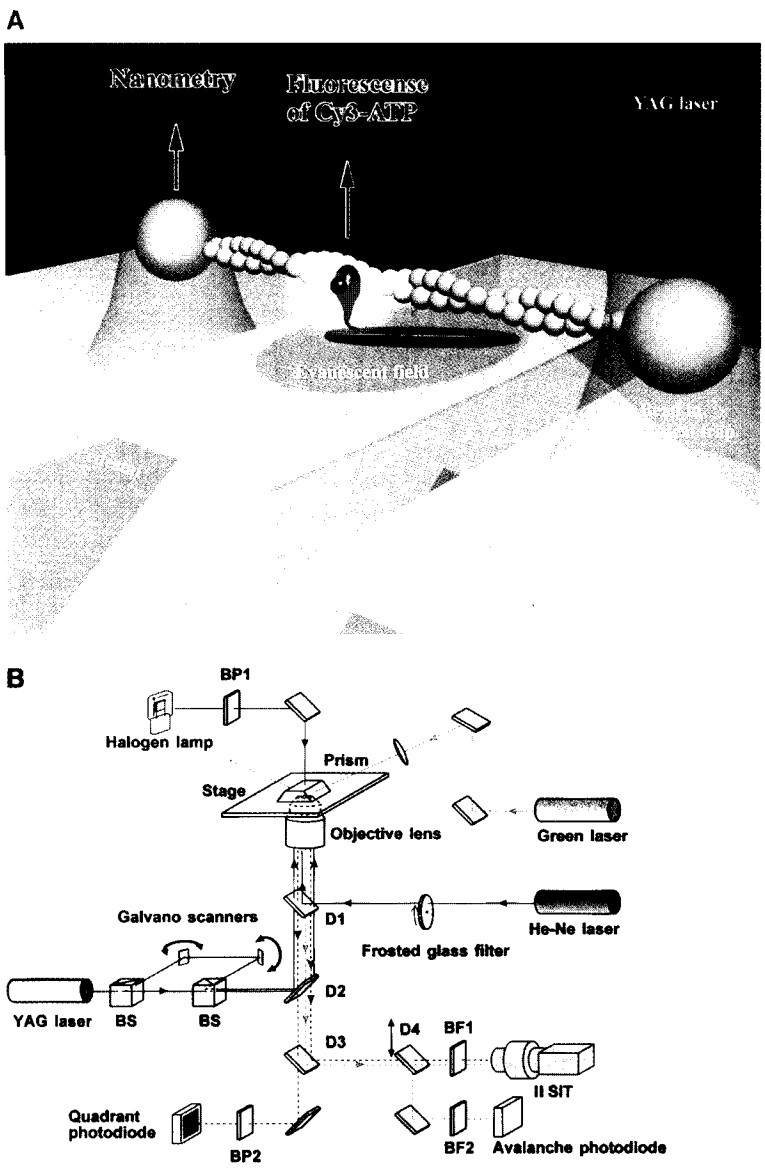

Figure 1. Simultaneous Measurement of Individual ATPase and Mechanical Reactions of Single One-Headed Myosin Molecules

(A) The experimental apparatus. A single actin filament with beads attached to both ends was suspended in solution by optical tweezers. The suspended actin filament was brought into contact with a single one-headed myosin molecule in a myosin-rod cofilament bound to the surface of a pedestal formed on a coverslip. Displacement or force due to actomyosin interactions was determined by measuring bead displacements with nanometer accuracy. Using total internal reflection fluorescence microscopy, individual ATPase reactions were monitored as changes in fluorescence intensity due to association-(hydrolysis)-dissociation events of a fluorescent ATP analog, Cy3-ATP, with the myosin head. The diagram has been drawn upside down. (B) Optics. See Microscopy (in Experimental Procedures) for details.

built on an inverted fluorescence microscope. Single actin filaments and cofilaments consisting of one-headed myosin and myosin rod fluorescently labeled with a red fluorescent dye Cy5 were observed under epifluorescence optics equipped with a He-Ne laser and a high sensitivity IISIT camera. Both ends of a single actin filament, approximately 15 μm long, were attached to beads via the biotin-avidin system, and the actin filament was captured and suspended in solution by manipulating the beads with dual optical tweezers generated by an infrared YAG laser (600 mW in max.). The suspended actin filament was brought into contact with a single one-headed myosin molecule in a myosin-rod cofilament bound to the surface of a rectangular pedestal approximately 7 μm wide and approximately 1 μm high, which had been formed on a glass surface by chemical etching.

The force and displacement caused by the myosin head were determined by measuring the displacement of the bead with nanometer accuracy (Finer et al., 1994). Individual ATPase reactions of single one-headed myosin molecules were measured by directly observing association-dissociation events of a fluorescent ATP analog labeled with Cy3 (Funatsu et al., 1995). The fluorescence was excited by the evanescent wave generated by total internal reflection of a green laser (532 nm, 2 mW) (Figure 1). The laser beam was incident on the interface between a fused silica coverslip (high reflective index) and the aqueous solution (low reflective index) at an angle greater than the critical angle for total internal reflection. This produced an evanescent field with a 1/e penetration depth of approximately 150 nm into the solution. The local illumination by the evanescent field greatly reduced the background luminescence so that it was at least 2000-fold lower than that of conventional epifluorescence microscopy and allowed single fluorophores to be clearly observed (Funatsu et al., 1995).

To measure the steps in the ATPase reaction, 10–20

nM Cy3-ATP was applied to myosin on the surface. The background fluorescence due to free Cy3-ATP in solution was sufficiently low to allow observation of fluorescent spots due to bound Cy3-ATP or Cy3-ADP. When Cy3-ATP or Cy3-ADP was associated with a myosin head on the surface, it appeared as a clearly defined localized fluorescent spot (Funatsu et al., 1995; Iwane et al., 1997; Tokunaga et al., 1997); free Cy3-nucleotides undergoing rapid Brownian motion, on the other hand, did not appear as discrete spots. Hence, by monitoring the repeated flickering of fluorescent spots due to Cy3-nucleotides bound to the myosin heads, individual nucleotide association-dissociation events could be detected. When the concentration of Cy3-ATP was increased to more than 50 nM, the fluorescent spots became obscure because of the high background fluorescence. Because the fluorescence intensity of Cy3-ATP is not greatly different from that of Cy3-ADP (Eccleston et al., 1996), the hydrolysis event itself could not be distinguished. However, as the affinity of myosin for ATP ($\sim 10^{11}$ M^{-1}) is much greater than that of ADP ($\sim 10^{6}$ M^{-1}) (Woledge et al, 1985; Goldman and Brenner 1987), the association-dissociation events of Cy3-nucleotide should correspond to the individual ATP turnover events. The averaged dissociation rate of Cy3-nucleotide from a myosin head is consistent with the Cy3-ATP turnover rate determined in solution (Funatsu, et al., 1993; Tokunaga et al., 1997). Therefore, the ATP turnover events can be detected by observing the association-dissociation events of Cy3-nucleotide. An IISIT camera and an avalanche photodiode (photon counter) were used for localizing bound nucleotides and measuring their fluorescence intensity, respectively.

Displacements in the Presence of ATP and Cy3-ATP

We tested whether force and displacement could be produced by myosin in the presence of Cy3-ATP as well as in the presence of ATP. Myosin consists of two heads, each of which has ATP and actin-binding sites. To simplify the assay, we have used one-headed myosin molecules prepared by papain digestion of skeletal muscle myosin. One-headed myosin moves actin as fast as intact (two-headed) myosin (Harada et al. 1987) and produces forces and displacements as large as those of intact myosin (Tanaka et al., 1997). In many previous in vitro motility models, individual mechanical events were measured from myosin subfragments, which were randomly bound to an artificial surface (Finer et al., 1994; Miyata et al., 1994; Molloy, et al., 1995; Guilford et al., 1997). The forces and displacements, however, strongly depend on the angle between the myosin and actin filaments (Ishijima et al., 1994; Tanaka et al., 1997). Therefore, to avoid effects of random orientation, we have measured the forces and displacements from single one-headed myosin molecules sparsely distributed in filaments copolymerized from one-headed myosin and headless myosin rods. These cofilaments were oriented within 30° relative to the actin filament axis. Cofilaments, synthesized by slowly mixing one-headed myosin with rods at a molar ratio of 1:1000, were 5–8 μm long and contained on average only one to two one-headed myosin molecules. Thus, the actin filament interacted with a single one-headed myosin molecule in the cofilament at a time (Figure 1A, refer to Figure 4). When the actin filament was brought into contact with the glass surface in the absence of myosin molecules, the Brownian motion of the bead did not change significantly, indicating that the actin filament did not interact with the glass surface to any significant degree.

Figure 2A shows a series of displacements caused by a single one-headed myosin molecule in the presence of 2 mM ATP. Sharp displacement spikes were observed. In intact muscle, such sharp displacement spikes should be developed. However, it was difficult to distinguish displacements caused by actomyosin interactions from Brownian motion of the beads. Therefore, in order to facilitate data analysis, the displacements were measured at low ATP or Cy3-ATP concentrations so that the durations of the mechanical events were long enough to be easily identified. Figures 2B and 2C (upper traces) show typical time courses for the generation of displacements in the presence of 100 nM ATP and 100 nM Cy3-ATP, respectively. Similar displacements were observed for the two nucleotides. The lower traces in Figures 2B and 2C show changes in the stiffness due to actin–myosin interactions, determined by measuring the variance of the bead position due to Brownian motion. The noise observed in the displacement traces is due mostly to Brownian motions at the low optical trap stiffness used. When the myosin head bound to the actin filament, the total stiffness of the system (including the trapped bead and the actomyosin bond) increased, and hence the Brownian motion of the bead decreased. The change in stiffness is an indicator of the interaction between the actin filament and the myosin head (Molloy et al., 1995).

Figure 3A shows a histogram (red bars) of the displacements in the presence of ATP, which have been scored using the increase in stiffness as the criterion for an actomyosin interaction. The displacements had a relatively broad distribution, which can be explained by the randomizing effect of the Brownian motions of the beads (Molloy, et al., 1995). In the absence of actomyosin interaction, optically trapped beads underwent large thermal vibrations around the equilibrium position (i.e., at zero displacement). Therefore, if a myosin head attached to the actin filament when the bead happened to be positioned at +30 nm from the equilibrium position and produced, for example, an active displacement of 20 nm, the observed displacement would be (20 + 30) nm = +50 nm. Conversely, if attachment occurred when the bead thermally moved to −30 nm, the observed displacement would be −10 nm. Thus, the spread of the distribution can be explained by Brownian motions and the position of the center of the distribution giving the displacement produced by the myosin head (Molloy et al., 1995). The displacement value determined from the center positions of the distributions (Figure 3A, red bars) was 15 nm, which was similar to that obtained in the presence of Cy3-ATP (12 nm, Figure 3B, red bars).

In the absence of ATP, the histogram (Figure 3A, green bars) also shows an approximate Gaussian distribution with a spread similar to that in the presence of ATP. However, the position of the center of the distribution was zero, indicating that the myosin head produced no force when it bound to an actin filament in the absence of ATP.

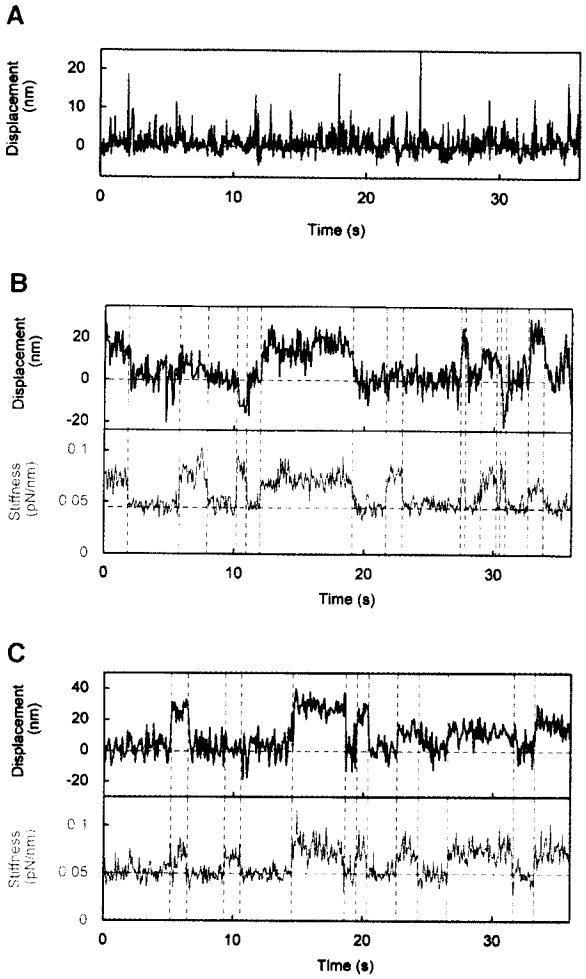

Figure 2. Individual Mechanical Events Produced by a Single One-Headed Myosin Molecule

(A) Time course of the displacements in the presence of 2 mM ATP. The trap stiffness was 0.15 pN/nm. The band width of a signal was 60 Hz.

(B and C) Time courses for the generation of displacements (upper traces) and changes in stiffness (lower traces) at 100 nM ATP (B) and 100 nM Cy3-ATP (C). The band width of each signal was 30 Hz. The stiffness was calculated from the variance of Brownian motions of the bead. The reciprocal variance is proportional to the stiffness. In all calculations of stiffness, data were passed through a low-pass filter with a band width of 12 kHz. The trap stiffness was 0.02 pN/nm in (B) and 0.05 pN/nm in (C). A 100 ms window was shifted every 50 ms, and the variance of the Brownian motions during each window was calculated. The dashed vertical lines mark the positions when the myosin heads interacted with an actin filament and generated displacements or detached. The positions of the dashed vertical lines were determined by cross-correlations between the data and a step function. The correlation function was calculated at a sampling rate of 120 Hz. The positions of the dashed horizontal lines were determined by averaging values in the ranges partitioned by the vertical lines. The vertical and horizontal lines shown in the remaining figures have all been determined using the same method. All experiments were performed in 25 mM KCl, 5 mM $MgCl_2$, 20 mM HEPES (pH 7.6) at 25°C. To reduce photobleaching, 50 μg/ml of glucose oxidase, 9 μg/ml catalase, 1.15 mg/ml glucose, and 0.5% 2-mercaptoethanol were added in the solution (Kishino and Yanagida, 1988; Harada et al., 1990).

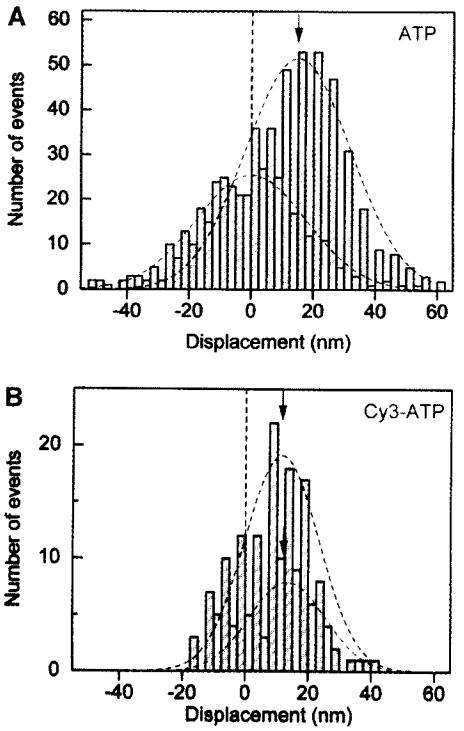

Figure 3. Displacements of Single One-Headed Myosin Molecules

(A) Histograms of the displacements in the presence of 100 nM ATP (red bars) and in the absence of ATP (green bars). The dashed lines indicate the Gaussian distributions with peaks at 15 nm (red bars) and 0 nm (green bars), and standard deviations (SD) of 17 nm (red bars) and 18 nm (green bars) have been fitted to the data. The total number of events counted were 437 (red bars) and 228 (green bars).

(B) Histogram (red bars) of the displacements concomitant with the release of nucleotide in the presence of 10 nM Cy3-ATP. The green bars show displacements produced between 0.1 and 1 s after the release of bound nucleotide (see Figure 7B and text for details). The dashed lines indicate the Gaussian distributions with peaks at 12 nm (red bars) and 13 nm (green bars). SD of 12 nm (red bars) and 12 nm (green bars) have been fitted to the data. The total number of events counted were 113 (red bars) and 48 (green bars). Arrows indicate the center of the distributions giving the average displacement caused by single myosin heads (see text). The displacements caused by the myosin heads were attenuated by the compliance (1/stiffness) of the actin/bead measurement system; the displacements were corrected as (observed displacements) × $(k_L + k_T)/k_L$, where k_L and k_T are the stiffness of the measurement system and optical trap, respectively (Svoboda and Block, 1994). The compliance of the measuring system is due predominantly to bonds between the actin filament and the beads and between the actin filament and the myosin head.

The second-order rate constants for the dissociation of actomyosin by ATP and Cy3-ATP have been estimated from the duration of the displacements. The average durations of displacements were 0.22 s at 1 μM and 2.0 s at 100 nM for ATP, and 3.0 s at 100 nM and 28 s at 10 nM for Cy3-ATP, giving second-order rate constants of approximately 5×10^6 $M^{-1}s^{-1}$ for ATP and approximately 3×10^6 $M^{-1}s^{-1}$ for Cy3-ATP. These values are very similar to those determined for ATP in solution (Woledge et al., 1985). The displacement and force values along with the association rate constant for Cy3-ATP with actomyosin are similar to those observed for ATP.

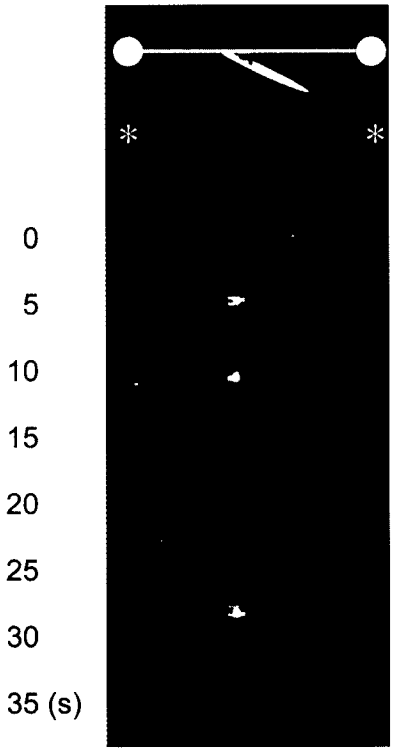

Figure 4. Individual Cy3-ATP Turnovers Produced by a Single One-Headed Myosin Molecule during Force Generation

(Top) Fluorescence image of a suspended actin filament interacting with a myosin-rod cofilament bound to a pedestal surface and a corresponding schematic drawing. Asterisks indicate the positions of the beads as observed under bright field illumination. Both filaments were labeled with Cy5.

(Bottom) The lower panels indicate sequential images of an association-(hydrolysis)-dissociation event of Cy3-ATP with the same myosin head within the filament shown above. Color has been altered for presentation purposes.

Simultaneous Measurements of Individual ATPase and Mechanical Reactions of Single Myosin Molecules

The upper two panels in Figure 4 show the fluorescence images of a single actin filament interacting with a single cofilament bound to the surface of the pedestal and a corresponding drawing. The lower panels in Figure 4 show fluorescence images of individual turnovers of Cy3-ATP molecules with a single one-headed myosin in the cofilament during an interaction with actin. All of the fluorescence intensities were similar (~1000 photons/s, see Figure 5), indicating that the fluorescent spots were due to single Cy3-ATP molecules. This result also indicates that no more than one myosin head was involved in the observation time.

Figure 5 shows traces of the mechanical and biochemical events recorded simultaneously (displacement, upper trace; stiffness changes due to actomyosin interactions, middle trace; and changes in the fluorescence intensity from bound Cy3-nucleotide, bottom trace). The stiffness, obtained from the variance of displacement due to Brownian motion of the bead, was a good indicator of interactions between the myosin head and the actin filament as mentioned above. The increase and decrease in the fluorescence intensity (bottom trace) are due to association and dissociation, respectively, of single Cy3-nucleotides with the myosin head. The return to zero displacement and the decrease in stiffness (i.e., dissociation of actomyosin rigor complexes) were associated with increases in the fluorescence intensity (i.e., association of Cy3-ATP to the myosin head). Changes in the displacement and increases in the stiffness (i.e., association of a myosin head with actin) were accompanied by decreases in the fluorescence intensity (i.e., dissociation of Cy3-nucleotide, presumably Cy3-ADP). Thus, we have directly detected the coupling between individual mechanical events and ATPase reactions at the single molecule level.

At 10–20 nM Cy3-ATP, displacements driven by the hydrolysis of Cy3-ATP, were maintained for tens of seconds until a new Cy3-ATP molecule bound to the myosin head. The displacement and the stiffness decreased upon binding of a new Cy3-ATP to the myosin head, which was due to the detachment of the myosin head from the actin filament. Figure 6A shows the displacement (upper trace), the change in the stiffness (middle trace), and the change in the fluorescence intensity due to Cy3-nucleotide binding to the myosin head (bottom trace) on an expanded time scale. When a Cy3-ATP nucleotide bound, the myosin head rapidly detached from actin. The spread of timings between the Cy3-ATP binding and the detachment of the myosin head was ±0.05 s (Figure 6B). As the dissociation of actomyosin upon binding of ATP should occur within 1 ms (Lymn and Taylor, 1971), the spread of the histogram shown in Figure 6B (0.05 s) should show the limits where the events are effectively detected.

Coupling between Displacement and the Release of Bound Nucleotide

Myosin heads, which had been detached from actin by binding of Cy3-ATP, reattached to the actin filament and generated force. The force generation was associated with the release of the bound Cy3-nucleotide, probably Cy3-ADP, but the timing was complex. Figures 7A and 7B show these events on an expanded time scale. In approximately 50% of events, nucleotide release coincided with force generation to within the time resolution of the system (Figure 7A). In the other events, nucleotide dissociated from free myosin heads, which reattached to the actin and generated displacements within approximately 1 s (Figures 7B and 7C). The histogram of the displacements produced after releasing Cy3-nucleotide (Figure 3B, green bars) showed an approximately Gaussian distribution with a peak at 13 nm from zero displacement. This indicates that the myosin heads could produce force and active displacements after the release of the bound nucleotide. If only rigor complexes were formed after release of nucleotide, then the distribution of displacements would have been centered at zero (Figure 3A, green bars).

Discussion

Motions of the actomyosin motor power the relative sliding between myosin and actin filaments (Huxley and

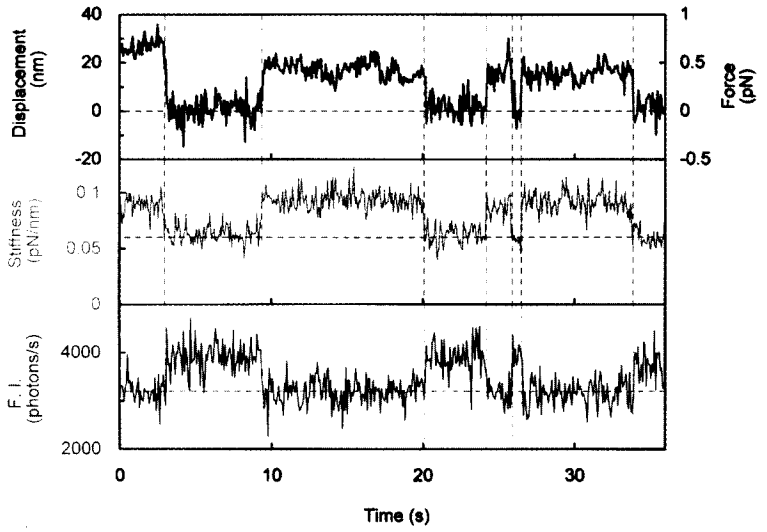

Figure 5. Simultaneous Measurements of Individual ATP Turnovers and Actomyosin Interactions by a Single Myosin Head

The upper and bottom traces show the time course of displacements and changes in fluorescence intensity from Cy3-nucleotide bound to the myosin head, respectively. The band width of each signal was 30 Hz. The ordinate of the bottom trace indicates the number of photons detected by an avalanche photodiode (Microscopy in Experimental Procedures). The middle trace shows changes in the stiffness (reciprocal of variance). A 100 ms window was shifted every 50 ms, and the variance of the Brownian motions during each window was calculated. The concentration of Cy3-ATP was 10 nM. The trap stiffness was approximately 0.05 pN/nm.

Hanson, 1954; Huxley and Niedergerke, 1954). In 1969, H. E. Huxley suggested that the sliding force is developed as a result of a change in the angle of attachment in the head part of a myosin cross-bridge attached to actin. Based on a mechanical investigation of muscle, Huxley and Simmons (1971) proposed a theoretical model, termed the "swinging cross-bridge model." Conformational changes in the myosin heads coupled to changes in bound ligands can be observed in crystals (Fisher et al., 1995), in solution (Wakabayashi et al., 1992), and in muscle fibers during contraction (Irving et al., 1992). The displacement expected from the observed conformational changes in the myosin head is approximately 6 nm, consistent with individual displacement events from single myosin subfragment-1 molecules measured using optical trapping nanometry (Molloy et al., 1995).

Our results, however, show that the myosin head produces a displacement of 15 nm. In this study, the effects of random orientation of myosin molecules and any damage of myosin molecules caused by interaction with the glass substrate have been minimized using copolymerized filaments (Ishijima et al., 1996; Tanaka et al., 1997). The large displacement observed in the present work is significant for understanding how conformational changes in the myosin head are involved in force generation. The myosin head may undergo several mechanical events during a single ATPase cycle (Yanagida, et al. 1985, 1993; Harada, et al., 1990; Higuchi and Goldman, 1991; Ishijima et al., 1991; Lombardi, et al., 1992). This finding will be discussed in further detail elsewhere (Tanaka et al., unpublished data; Kitamura et al., unpublished data).

The elementary steps of the actomyosin ATPase have been extensively characterized in biochemical experiments using the isolated proteins in solution, and the kinetic pathway was related to the swinging cross-bridge model (Lymn and Taylor, 1971; Tonomura, 1972; Trentham et al., 1976; Eisenberg et al., 1980). Kinetic studies show that in the absence of actin, ATP is hydrolyzed into ADP and, in a stable intermediate complex, myosin-ADP-Pi (M-ADP-Pi). Release of Pi and ADP from M-ADP-Pi is greatly accelerated in the presence of actin (Lymn and Taylor, 1971; Tonomura, 1972). Furthermore, basic free energy greatly decreases upon release from AM-ADP-Pi (Kodama, 1985), suggesting that the force develops on release of Pi and/or ADP (Lymn and Taylor, 1971):

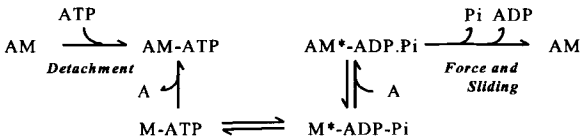

where A represents actin and the asterisk (*) indicates high free energy states of a myosin head (Kodama, 1985).

Recently, the three dimensional atomic structure of a myosin head has been resolved (Rayment et al., 1993a), allowing a more detailed structural analysis of the swinging cross-bridge model based on the kinetic scheme (Rayment et al., 1993b; Fisher et al., 1995). There is, however, no direct evidence for tight coupling between the mechanical and chemical reactions, because the ATPase reaction of single actomyosin complexes was not previously measured during force generation.

We have succeeded in simultaneously measuring individual mechanical and ATPase reactions of myosin during force generation at the single molecule level. Myosin heads produced force promptly when the bound nucleotide was released (Figure 7A), which may be consistent with the above kinetic scheme. Some myosin heads, however, produced force several hundred milliseconds after the fluorescence intensity from bound Cy3-nucleotide had decreased (Figures 7B and 7C). The decrease in the fluorescence intensity shown in Figure 7B, however, may be due to photobleaching as well as the dissociation of the bound Cy3-nucleotide. The photobleaching rate of Cy3-ATP bound to a glass surface was 0.008 $\pm$ 0.002 s^{-1} under conditions when 1000 photons/s were collected by the detector. Upon binding to a myosin head in the presence of vanadate, the photobleaching rate of Cy3-ADP did not change. The actomyosin association rate constant, obtained from the durations of intervals when myosin heads with bound nucleotide were

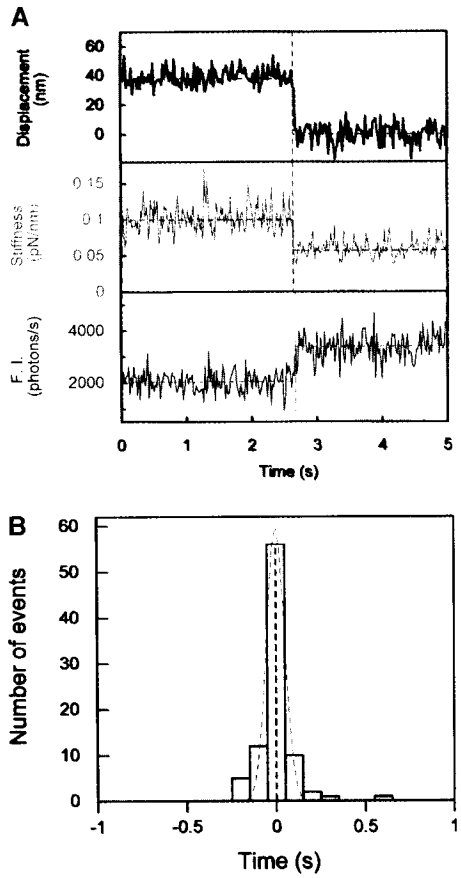

Figure 6. Time Course of Detachment of a Myosin Head upon Binding of Cy3-ATP

(A) The time courses of detachment of a myosin head from an actin filament (upper trace) and association of Cy3-ATP with the myosin head (bottom trace) in the presence of 10 nM Cy3-ATP plotted on an expanded time scale. The band width of each signal was 120 Hz. The middle trace shows the changes in stiffness. A 30 ms window was shifted every 15 ms, and the variance of the Brownian motions of the bead during each window was calculated.

(B) A histogram of the time delays between detachment of a myosin head and the binding of Cy3-ATP. The dashed line indicates the Gaussian distribution with a peak at 0 nm and a SD of 0.05 s fitted to the data as described previously (Higuchi et al, 1997). Total number of events counted, 87.

dissociated from an actin filament, was approximately 0.13 s^{-1}. Therefore, the probability that photobleaching occurred prior to nucleotide release was as follows: $\sim 1 - \exp(-0.008 s^{-1}/0.13 s^{-1}) = \sim 6\%$. Thus, the observed decrease in the fluorescence intensity is most often ($\sim$94%) due to the dissociation of the bound Cy3-nucleotides. Several other possible artifacts are also unlikely. The concentration of contaminating ATP was low ($<$5% of Cy3-ATP, Experimental Procedures). Photobleaching of free Cy3-ATP in solution during experiments should be negligible, because the illumination volume was 5×10^6-fold smaller than the total volume and the diffusion of Cy3-ATP was very rapid ($\sim$1 μm/ms). Cy3-ATP binding and prompt (< 0.05 s) force generation during the observed delay times ($<$1 s) is unlikely considering that the second-order rate constant for binding of

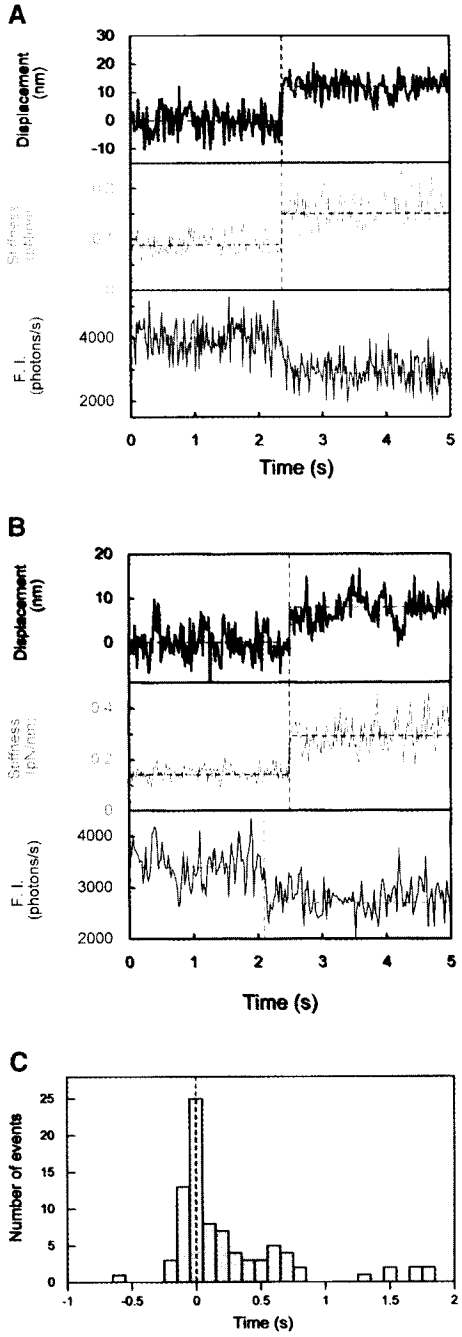

Figure 7. The Time Courses of Displacement Generation and the Release of Cy3-Nucleotide

(A) The generation of a displacement coincided with the release of Cy3-nucleotide (probably Cy3-ADP).

(B) The displacement was delayed after the release of Cy3-nucleotide. Traces indicate the time courses of displacement generation (upper) and changes in the fluorescence intensity from the Cy3-nucleotide (bottom). The band width of each signal was 120 Hz. The stiffness (middle trace) was calculated as described in the legend of Figure 6A. The concentration of Cy3-ATP is 10 nM. (C) Histogram showing the delay times from the release of Cy3-nucleotide to the generation of displacements. Total counted events, 85.

Cy3-ATP to myosin is 10^6–10^7 $M^{-1}s^{-1}$ (Eccleston et al., 1996), and therefore the association rate for Cy3-ATP with myosin is 0.01–0.1 s^{-1} at 10 nM (= 10^6–10^7 $M^{-1}s^{-1} \times$ 10 nM). Instability in the fluorescence intensity, termed "blinking," which has been reported for other fluorophores (Ha et al., 1996; Dickson et al., 1997), was not observed with Cy3-nucleotides bound to the myosin heads (Figures 5, 6A, 7A, and 7B). Thus, our results show that the force can be generated several hundred milliseconds after the release of bound nucleotide from the myosin head.

The following kinetic scheme is consistent with our findings:

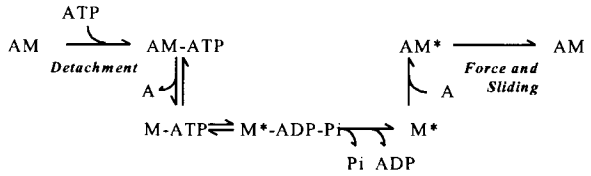

From a thermodynamic viewpoint, as the free energy level of the A + M state is higher than that of AM, it is possible that the myosin head can produce force when it binds to actin in the absence of ATP (Eisenberg et al., 1980; Geeves et al., 1984). In this case, ATP would be used for dissociation of the myosin head from actin. However, the myosin head produced no force upon binding to actin in the absence of ATP (Figure 3A, green bars). Therefore, our results suggest that the myosin head can store chemical energy derived from ATP hydrolysis and can generate force several hundred milliseconds after the release of ADP and Pi (Figure 7C).

Is such a prolonged hysteresis or memory effect possible? It is known that some enzymes, termed hysteretic enzymes (e.g., phosphorylase from frog muscle), respond slowly (in seconds to minutes) to rapid changes in ligand concentration. Kinetic analysis has suggested that the enzymes can exist in two or more different conformational states, and slow transitions among those states lead to the hysteretic behavior (Frieden, 1970). Recently, we have been able to directly observe the conformational states of individual protein molecules (troponin, a calcium-signaling protein) by single molecule fluorescence resonance energy transfer imaging (Ishii et al., 1997). The results have strongly suggested that some proteins exist in multiple conformational states coupled through slow transitions in the time range of seconds. The chemical energy liberated by ATP hydrolysis could be stored in such a long-lived conformational state in the myosin head.

In the present work, we observed the force generation several hundred milliseconds after the release of ADP from the myosin head. In intact muscle, the force generation would not be delayed for so long, because the myosin head is closely surrounded by actin filaments and would bind more rapidly to the actin filaments. This difference in time, however, is not significant. The most important feature is which step in the ATPase reaction is related to the force generation. Furthermore, one may argue that the myosin head rapidly rebinds ATP after releasing bound ADP at saturating ATP concentrations. This suggests that the hysteresis state is not important in intact muscle. This argument is not necessarily correct because it is likely that the myosin head after releasing bound ADP, which stores the chemical energy, does not rebind ATP before generation force. Kinetic studies have suggested that some metabolic enzymes show hysteretical response to rapid changes in ligand concentration (Frieden, 1970).

In the above argument, we assume that the release of Pi from myosin precedes that of ADP. Many investigations have supported this assumption, but there has been no definite evidence to support this (Bagshaw and Trentham, 1974; Woledge et al., 1985; Goldman, 1987; Brune et al., 1994). Therefore, the possibility cannot be completely excluded that the force generation may be coupled to the release of Pi.

The present technique could be extended to study other allosteric enzymes, such as GTP-binding cell signaling proteins, to examine if high energy states or signals can be retained after ligand changes. This hysteresis or memory effect may be a common characteristic of the protein molecules and important for regulation of complex kinetic pathways in which many enzymes or signaling proteins are involved cooperatively.

Experimental Procedures

Preparation of Proteins

Myosin and actin were obtained from rabbit skeletal muscle. Myosin was extracted from muscle and purified (Harada et al., 1990). Myosin molecules were heavily digested with papain to produce one-headed myosin, myosin head (S1), and rod (Harada et al., 1987). Myosin heads were removed from the digested sample and one-headed myosin and rod mixture obtained. Rods were not removed because filaments copolymerized from one-headed myosin and rod were used in the experiments. Myosin rods were prepared from rabbit skeletal myosin by digestion with α-chymotrypsin (Margossian and Lowey, 1982).

The purity of the one-headed myosin preparation was checked by 3% polyacrylamide gel electrophoresis (PAGE) according to the method of Harada et al. (1987). The purity was also checked by observing images of rotary-shadowed molecules by electron microscopy (Harada et al., 1990; Tanaka, et al., 1997). The contaminating two-headed myosin was less than 2% of one-headed myosin.

Myosin-Rod Cofilament

One-headed myosin and rods were mixed to form copolymerized filaments, and the cofilaments were bound to a glass surface as previously described (Ishijima et al., 1996). The total concentration of the proteins was set to 0.15 μM, and the molar ratio of myosin to myosin rod in the mixture was adjusted 1:1000. 1% Cy5-labeled rod was included in order to visualize the cofilament. One-headed myosin-rod cofilaments, 5–8 μm long, were obtained in which one to two one-headed myosin molecules were distributed on average. The number of one-headed myosin molecules in the cofilament could be easily counted by observing bound Cy3-ATP molecules (see Figure 4).

Fluorescently Labeled and Biotinylated Actin Filaments

To visualize and attach the actin filaments to the beads, actin filaments were fluorescently labeled and biotinylated. Reactive Cys 374 of actin was labeled with the fluorescent dye, Cy5-maleimide. Cy5-maleimide was synthesized from Cy5-NHS (FluoroLink Cy5 Monofunctional Dye, Amersham) (λ_{ex}, 650 nm; λ_{em}, 670 nm) by incubation with PEM (Dojindo) for 8 hr at 40°C. Actin filaments were mixed with Cy5-maleimide in a monomer: probe ratio of 1:10 at 25°C for 1 hr. Unbound dye was washed out by repeated centrifugations, and Cy5-labeled actin filaments were depolymerized in G buffer (0.1 mM ATP, 0.2 mM $CaCl_2$, 10 mM HEPES, [pH 7.8]). The molar ratio of Cy5 to actin monomer was approximately 0.5:1.

Biotinylated actin was prepared by linking biotin-$PEAC_5$-maleimide (Dojindo) to Cys 374 of actin as follows: actin filaments and biotin-$PEAC_5$-maleimide were mixed in a molar ratio of 1:5 at 25°C for 1 hr. Unbound biotin-$PEAC_5$-maleimide was washed out by repeated centrifugations and biotinylated actin filaments were depolymerized in the G buffer. Actin filaments were obtained by mixing native actin, the Cy5-labeled actin, and the biotinylated-actin sample at molar ratio of 5:4:1 in F buffer (0.1 M KCl, 10 mM HEPES, [pH 7.8]). Contaminating ATP was removed by gel filtration (Clontech, CHROMA SPIN-10) just before polymerization. The ATP concentration of the eluted solution was determined by measuring the concentration of Pi with a Malachite green method (Ohno and Kodama, 1991) after hydrolysis in the presence of apyrase (10 U). The concentration was less than 5 μM. In the experiments, the solution was diluted 10,000-fold so the concentration of nonfluorescent ATP was less than 0.5 nM, which was at least 20-fold lower than the concentration of Cy3-ATP (10–20 nM) used.

Biotinylated Beads

To attach a biotinylated actin filament to beads using the biotin-streptavidin system, the beads were biotinylated as follows: 500 μl of 2% (w/v) polystyrene latex beads with carboxylate groups on their surface (Uniform Microspheres, Bangs Laboratories; 0.945 μm in diameter) were mixed with 50 μl of 1 mg/ml biotin-X-cadaverine (Molecular Probes) in the presence of 20 mM phosphate buffer (pH 7.0) and 20 mM EDC (PIERCE), and the mixture was incubated for 30 min at 25°C. The free biotin-X-cadaverine and EDC were washed out by repeated centrifugations. The biotinylated beads were suspended in 500 μl of 20 mM phosphate buffer (pH 7.0) and mixed with 25 μl of 10 mg/ml streptavidin (Molecular Probes). After incubation for 30 min at 25°C, the beads were washed by three repeated centrifugations to remove free streptavidin. They were then coated with BSA (incubation in 1 mg/ml BSA solution) to avoid absorption of the beads onto the glass surface.

Cy3-ATP

Cy3-ATP, in which the Cy3 was coupled to the ribose ring, was synthesized and purified as previously described (Tokunaga, et al., 1997). The purity was greater than 99% as determined by an FPLC anion-exchange chromatography on Mono Q (Pharmacia). The rates of photobleaching of the Cy3-nucleotides were measured when Cy3-ATP was bound to a glass surface and Cy3-ADP formed a stable complex with a myosin head in the presence of 1 mM vanadate (Goodno, 1979) at the same medium condition and temperature as those used in these experiments.

Chemical Etching of a Coverslip

To raise the myosin-rod cofilaments higher than the bead radius (see Figure 1A), pedestals were made on a glass surface by chemical etching of the coverslips. Coverslips (fused silica, 26 mm × 55 mm in area, 0.8 mm in thickness, Matsunami, Japan) were cleaned by washing in 0.1 M KOH and 100% ethanol. The clean surface was coated with chrome by vacuum evaporation and then coated with photoresist (AZ RFP210K, Hoechst, Japan). Striped patterns were printed on the surface by irradiating a UV light through a striped pattern mask (width, 10 μm). The resist film was developed, and the irradiated area was removed (AZ developer, Hoechst). The chrome unprotected by remaining resist was removed with a chrome etching solution (7.5 wt% $HClO_4$, 12.1 wt% $(NH_4)_2Ce(NO_3)_6$, 80.4 wt% H_2O), and the bare surfaces of the coverslip were etched in a solution containing 3% NH_4F and 50% H_2SO_4 for 15 min at 25°C. The etched coverslips were rinsed with water, and the remaining chrome on the surface was removed with the chrome etching solution. This method produced pedestals on the glass surface approximately 7 μm wide and 1 μm deep.

Microscopy

Imaging and Photon Counting

An inverted fluorescence microscope (TMD-300, Nikon, Japan) and other optics were set on a vibration-free table (TDI-189LA, HELTZ, Japan). Cy5-labeled myosin-rod cofilaments and Cy5-labeled actin filaments were observed by epifluorescence microscopy. A beam of a He-Ne laser (GLG5360, NEC; power 5 mW; λ, 632.8 nm) was passed through a quarter-wave plate and a rotating frosted glass to obtain homogeneous illumination. The beam was directed to an oil immersion objective (fluor 100×, NA1.30, NIKON) by a dichroic mirror that reflected laser beams of 532 and 632.8 nm and passed fluorescence of Cy3 and Cy5 (D1 in Figure 1B; Sigma Koki, Japan). Background luminescence and infrared light for nanometry were rejected with a barrier filter (BF1, 670DF40 for Cy5 or 570DF30 for Cy3, Omega Optical, VT). The fluorescent images of the filaments (λ_{em}, ~670 nm) were captured by a SIT camera (C2400-08, Hamamatsu Photonics, Japan), coupled to an image intensifier (VS4-1845, Videoscope, VA), and displayed on a TV monitor.

Cy3-nucleotide (ATP or ADP) was observed with total internal reflection fluorescence microscopy. A beam of a frequency-doubled Nd:YAG green laser (model 142-532-100, Light Wave; λ, 532 nm) was incident on a fused silica slide, parallel to the longitudinal axis of striped pedestals, through a trapezoidal fused silica prism. The gap between the prism and a fused silica slide was filled with pure glycerol. The incident angle at the quartz-to-solution interface was 75° to the normal (the critical angle, 66°). The beam was focused to 40 × 160 μm^2at the specimen plane by a lens. The power was 2 mW at the specimen plane. Scattering of the incident light by the edge of pedestals was sufficiently small to observe single fluorophores.

The fluorescence image of Cy3-nucleotide (λ_{em}, ~570 nm) of fluorescence intensity of Cy3-nucleotides bound to myosin was captured by the high sensitivity camera as described above. An avalanche photodiode (SPCM-200PQ, EG and G; quantum efficiency, 40% at 570 nm) was used for quantitative analysis of fluorescence intensity. Fluorescence from circular area limited to 0.7 μm in diameter was detected to minimize the background. A dichroic mirror reflected fluorescence of Cy3 and passed that of Cy5 (D4 in Figure 1B; separation wave length of 630 nm; Sigma, Koki). Background luminescence, scattered light from the He-Ne laser, and infrared light for nanometry were rejected with a barrier filter (BF2 in Figure 1B; 570DF30, Omega Optical). The configuration of these optics enabled us to count photons from Cy3-nucleotide while observing the actin and cofilaments. The number of photons was converted to voltage every 2 ms by a F-V converter (CF101FV, Sentech, Japan), and the output was recorded on magnetic tape by a digital data recorder (RD-101T, TEAC, Japan) at a sampling rate of 24 kHz. The data were analyzed by a signal processor (R9211A, Advantest, Japan) and a personal computer (FM-V, Fujitsu, Japan).

Optical Tweezers and Nanometry

Two optical traps were generated by an infrared YAG laser (T10-8S, Spectraphisics, CA; power, 600 mW in max; λ, 1064 nm) reflected by a dichroic mirror (D2 in Figure 1B). The laser beam was passed through a quarter-wave plate followed by two polarizing beam splitters (BS in Figure 1B). The position of one beam was fixed. The position of the other one was adjusted by two orthogonal galvano scanners (G120DT, General Scanning, Japan) controlled by a computer. The force produced by a myosin head was determined by measuring the displacement of a bead attached to actin from the center of the optical trap. The force is proportional to the displacement of the bead from the center (Simmons et al. 1993; Svoboda et al. 1993). The equivalent spring constant of trapped beads, proportional to the laser power, was very small (0.02–0.06 pN/nm) at the present condition so the beads experienced Brownian motions within the trap at the peak-to-peak amplitudes of tens of nanometers. The equivalent spring constant (k) of the trapped bead was determined from these Brownian motions using the equipartition law, $1/2k < x^2 > = 1/2K_BT$ (Landaou and Lifshitz, 1969).

The bead displacements were measured with nanometer accuracy as follows. Microbeads were illuminated with infrared light from a halogen lamp that passed through a band pass filter (BP1 in Figure 1B; 750-950 nm, Asahi Bunko, Japan). The infrared light passed through the dichroic mirror with a separation wavelength of 750 nm (D3 in Figure 1B, Sigma Koki). The image of the bead was projected onto the center of a quadrant photodiode detector (S994-13, Hamamatsu Photonics). The band pass filter of 750–950 nm was used to eliminate the light from a visible laser and an infrared YAG laser (BP2 in Figure 1B). The outputs from the quadrant photodiode were converted into voltage by I-V converters (AD-11, Analog Devices, Japan). Displacements of the bead in orthogonal directions were determined from the differential outputs of the quadrant photodiode

amplified by an order-made differential amplifier (OP711A, Sentech, Japan). The differential output of the quadrant photodiode was recorded on digital tape along with the fluorescence intensity from the Cy3-nucleotides and analyzed as described above.

Acknowledgments

We wish to thank Dr. Y. E. Goldman, Dr. C. Bagshaw, Dr. J. Wray, Dr. A. Inoue, and Dr. J. West for critically reading the manuscript and for their valuable suggestions. We are grateful to Dr. K. Oiwa and Dr. D. Trentham for their comments on Cy3-nucleotides. We also thank the members of ERATO Biomotron project for their discussion and critical comments on the manuscript.

Received October 20, 1997; revised, December 15, 1997.

References

Bagshaw, C.R., and Trentham, D.R. (1974). The characterization of myosin-product complexes and of product release steps during the magnesium ion-dependent adonosine triphosphate reaction. Biochem. J. *141*, 331–349.

Brune, M., Hunter, J.L., Corrie, J.E., and Webb, M.R. (1994). Direct, real-time measurement of rapid inorganic phosphate release using a novel fluorescent probe and its application to actomyosin subfragment 1 ATPase. Biochemistry *33*, 8262–8271.

Conibear, P.B., Jeffreys, D.S., Seehra, C.K., Eaton, R.J., and Bagshaw, C.R. (1996). Kinetic and spectroscopic characterization of fluorescent ribose-modified ATP analogs upon interaction with skeletal muscle myosin subfragment 1. Biochemistry *35*, 2299–2308.

Dickson, R.M., Cubitt, A.B., Tsien, R.Y., and Moerner, W.E. (1997). On/off blinking and switching behaviour of single molecules of green fluorescent protein. Nature *24*, 355–358.

Eccleston, J.F., Oiwa, K., Ferenczi, M.A., Anson, M., Corrie, J.E.T., Yamada, A., Nakayama, H., and Trentham, D.R. (1996). Ribose-linked sulfoindocyanine conjugates of ATP: Cy3-EDA-ATP and Cy5-EDA-ATP. Biophys. J. *70*, A159.

Eisenberg, E., Hill, T.L., and Chen, Y. (1980). Cross-bridge model of muscle contraction: quantitative analysis. Biophys. J. *29*, 195–227.

Finer, J.T., Simmons, R.M., and Spudich, J.A. (1994). Single myosin mechanics: piconewton forces and nanometre steps. Nature *368*, 113–119.

Fisher, A.J., Smith, C.A., Thoden, J.B., Smith, R., Sutoh, K., Holden, H.M., and Rayment, I. (1995). X-ray structures of the myosin motor domain of Dictyostelium discoideum complexed with MgADP-BeFx and MgADP-AlF4-. Biochemistry *34*, 8960–8972.

Frieden, C. (1970). Kinetic aspects of regulation of metabolic processes: the hysteretic enzyme concept. J. Biol. Chem. *245*, 5788–5799.

Funatsu, T., Harada, Y., Tokunaga, M., Saito, K., and Yanagida, T. (1995). Imaging of single fluorescent molecules and individual ATP turnovers by single myosin molecules in aqueous solution. Nature *374*, 555–559.

Geeves, M.A., Goody, R.S., and Gutfreund, H. (1984). Kinetics of acto-S1 interaction as a guide to a model for the crossbridge cycle. J. Muscle Res. Cell Motil. *5*, 351–361.

Goldman, Y.E. (1987). Kinetics of the actomyosin ATPase in muscle fibers. Annu. Rev. Physiol. *49*, 637–654.

Goldman, Y.E., and Brenner, B. (1987). Special topic: molecular mechanism of muscle contraction. General introduction. Annu. Rev. Physiol. *49*, 629–636.

Goodno, C.C. (1979). Inhibition of myosin ATPase by vanadate ion. Proc. Natl. Acad. Sci. USA *76*, 2620–2624.

Guilford, W.H., Dupuis, D.E., Kennedy, G., Wu, J., Patlak, J.B., and Warshaw, D.M. (1997). Smooth muscle and skeletal muscle myosins produce similar unitary forces and displacements in the laser trap. Biophys. J. *72*, 1006–1021.

Ha, T., Enderle, T., Ogletree, D.F., Chemla, D.S., Selvin, P.R., and Weiss, S. (1996). Probing the interaction between two single molecules: fluorescence resonance energy transfer between a single donor and a single acceptor. Proc. Natl. Acad. Sci. USA *93*, 6264–6268.

Harada, Y., Noguchi, A., Kishino, A., and Yanagida, T. (1987). Sliding movement of single actin filaments on one-headed myosin filaments. Nature (London). *326*, 805–808.

Harada, Y., Sakurada, K., Aoki, T., Thomas, D.D., and Yanagida T. (1990). Mechanochemical coupling in actomyosin energy transduction studied by in vitro movement assay. J. Mol. Biol. *216*, 49–68.

Harada, Y., Funatsu, T., Tokunaga, M., Saito, K., Higuchi, H., Ishii, Y., and Yanagida, T. (1997). Single molecule imaging and nanomanipulation of biomolecules. Meth. Cell Biol. *55*, 117–128.

Higuchi, H., and Goldman, Y.E. (1991). Sliding distance between actin and myosin filaments per ATP molecule hydrolysed in skinned muscle fibers. Nature *352*, 352–354.

Higuchi, H., Muto, E., Inoue, Y., and Yanagida, T. (1997). Kinetics of force generation by single kinesin molecules activated by laser photolysis of caged ATP. Proc. Natl. Acad. Sci. USA *94*, 4395–4400.

Huxley, A.F., and Niedergerke, R.M. (1954). Interference microscopy of living muscle fibers. Nature *173*, 971–973.

Huxley, A.F., and Simmons, R.M. (1971). Proposed mechanism of force generation in striated muscle. Nature *233*, 533–538.

Huxley, H.E., and Hanson, J. (1954). Changes in the cross-striations of muscle during contraction and stretch and their structural interpretation. Nature *173*, 973–976.

Huxley, H.E. (1969). The mechanism of muscular contraction. Science *164*, 1356–1366.

Huxley, H.E. (1990). Sliding filaments and molecular motile systems. J. Biol. Chem. *265*, 8347–8350.

Irving, M., Lombardi, V., Piazzesi, G., and Ferenczi, M.A. (1992). Myosin head movements are synchronous with the elementary force-generating process in muscle. Nature *357*, 156–158.

Ishii, Y., Funatsu, T., Wazawa, T., Yoshida, T., Watai, J., Ishii, M., and Yanagida, T. (1997). Communication between troponin-C and -I revealed by single molecule fluorescence spectroscopy and FRET. Biophys. J. *72*, A283.

Ishijima, A., Doi, T., Sakurada, K., and Yanagida, T. (1991). Subpiconewton force fluctuations of actomyosin in vitro. Nature *352*, 301–306.

Ishijima, A., Harada, Y., Kojima, H., Funatsu, T., Higuchi, H., and Yanagida, T. (1994). Single-molecule analysis of the actomyosin motor using nano-manipulation. Biochem. Biophys. Res. Commun. *199*, 1057–1063.

Ishijima, A., Kojima, H., Higuchi, H., Harada, Y., Funatsu, T., and Yanagida, T. (1996). Multiple- and single-molecule analysis of the actomyosin motor by namometer-piconewton manipulation with a microneedle: unitary steps and force. Biophys. J. *70*, 383–400.

Iwane, A.H., Funatsu, T., Harada, Y., Tokunaga, M., Ohara, O., Morimoto, S., and Yanagida, T. (1997). Single molecule assay of individual ATP turnover by a myosin-GFP fusion protein expressed in vitro. FEBS Lett. *407*, 235–238.

Kishino, A., and Yanagida, T. (1988). Force measurements by micromanipulation of a single actin filament by glass needles. Nature *334*, 74–76.

Kodama, T. (1985). Thermodynamic analysis of muscle ATPase mechanics. Physicol. Rev. *65*, 467–551.

Kron, S.J., and Spudich, J.A. (1986). Fluorescent actin filaments move on myosin fixed to a glass surface. Proc. Natl. Acad. Sci. USA *83*, 6272–6276.

Landaou, L., and Lifshitz, E.M. (1969). Chapter 4. In Statistical Physics. (Oxford: Pergamon), 111–157.

Lombardi, V., Piazzesi, G., and Linari, M. (1992). Rapid regeneration of the actin-myosin power stroke in contracting muscle. Nature (London) *355*, 638–641.

Lymn, R.W., and Taylor, E.W. (1971). Mechanism of adenosine triphosphate hydrolysis by actomyosin. Biochemistry *10*, 4617–4624.

Margossian, S.S., and Lowey, S. (1982). Preparation of myosin and its subfragments from rabbit skeletal muscle. Meth. Enzymol. *85*, 55–71.

Miyata, H., Hakozaki, H., Yoshikawa, H., Suzuki, N., Kinoshita, K.,

Jr., Nishizaka, T., and Ishiwata, S. (1994). Stepwise motion of an actin filament over a small number of heavy meromyosin molecules is revealed in an in vitro motility assay. J. Biochem. *115*, 644–647.

Molloy, J.E., Burns, J.E., Kendrick-Jones, J., Tregear, R.T., and White, D.C.S. (1995). Movement and force produced by a single myosin head. Nature *378*, 209–212.

Monod, J., Wyman, J., and Changeux, J.-P. (1965). On the nature of allosteric transitions: a plausible model. J. Mol. Biol. *12*, 88–118.

Ohno, T., and Kodama, T. (1991). Kinetics of adenosine triphosphate hydrolysis by shortening myofibrils from rabbit psoas muscle. J. Physiol. *441*, 685–702.

Rayment, I., Rypniewski, W.R., Schmidt-Base, K., Smith, R., Tomchick, D.R., Benning, M.M., Winkelmann, D.A., Wesenberg, G., and Holden, H.M. (1993a). Three-dimensional structure of myosin subfragment-1: a molecular motor. Science *261*, 50–58.

Rayment, I., Holden, H.M., Whittaker, M., Yohn, C.B., Lorentz, M., Holmes, K.C., and Milligan, R.A. (1993b). Structure of the actin-myosin complex and its implications for muscle contraction. Science *261*, 58–65.

Simmons, R.M., Finer, J.T., Warrick, H.M., Kralik, B., Chu, S., and Spudich, J.A. (1993). Force on single actin filaments in a motility assay measured with an optical trap. In Mechanism of Myofilament Sliding in Muscle Contraction. H. Sugi and G.H. Pollack, eds. (New York: Plenum), pp. 331–336.

Svoboda, K., Schmidt, C.F., Schnapp, B.J., and Block, S.M. (1993). Direct observation of kinesin stepping by optical trapping interferometry. Nature *365*, 721–727.

Svoboda, K., and Block, S.M. (1994). Forces and velocities measured for single kinesin molecules. Cell *77*, 773–784.

Tanaka, H., Ishijima, A., Honda, M., Saito, K., and Yanagida, T. (1997). Orientation-dependent displacements by single one-headed myosin molecules in a synthetic myosin cofilament. Biophys. J. *72*, A55.

Tokunaga, M., Kitamura, K., Saito, K., Iwane, A.H., and Yanagida, T. (1997). Single molecule imaging of fluorophores and enzymatic reactions achieved by objective type total internal reflection fluorescence microscopy. Biochem. Biophys. Res. Commun. *235*, 47–53.

Tonomura, Y. (1972). Muscle Proteins, Muscle Contraction and Cation Transport. (Tokyo and Baltimore: Tokyo and University Park).

Toyoshima, Y.Y., Kron, S.J., McNally, E.M., Niebling, K.R., Toyoshima, C., and Spudich, J.A. (1987). Myosin subfragment-1 is sufficient to move actin filaments in vitro. Nature *328*, 536–539.

Trentham, D.R., Eccleston, J.F., and Bagshaw, C.R. (1976). Kinetic analysis of ATPase mechanisms. Q. Rev. Biophys. *9*, 217–281.

Vale, R.D., Funatsu, T., Pierce, D.W., Romberg, L., Harada, Y., and Yanagida, T. (1996). Direct observation of single kinesin molecules moving along microtubules. Nature *380*, 451–453.

Wakabayashi, K., Tokunaga, M., Kohno, I., Sugimoto, Y., Hamanaka, T., Takezawa, Y., Wakabayashi, T., and Amemiya, Y. (1992). Small-angle Synchrotron X-ray scattering reveals distinct shape changes of the myosin head during hydrolysis of ATP. Science *258*, 443–447.

Woledge, R.C., Curtin, N.A., and Homsher, E. (1985). Energy aspects of muscle contraction. Monogr. Physiol. Soc. *41*, 119–165.

Yanagida, T., Nakase, M., Nishiyama, K., and Oosawa, F. (1984). Direct observation of motion of single F-actin filaments in the presence of myosin. Nature *307*, 58–60.

Yanagida, T., Arata, T., and Oosawa, F. (1985). Sliding distance of actin filament induced by a myosin crossbridge during one ATP hydrolysis cycle. Nature *316*, 366–369.

Yanagida, T., Harada, Y., and Ishijima, A. (1993). Nano-manipulation of actomyosin molecular motors in vitro: a new working principle. Trends Biochem. Sci. *18*, 319–324.

Yount, R.G., Lawson, D., and Rayment, I. (1995). Is myosin a "back door" enzyme? Biophys. J. *68*, 44S–47S.